Journal of Materials Chemistry C

Accepted Manuscript

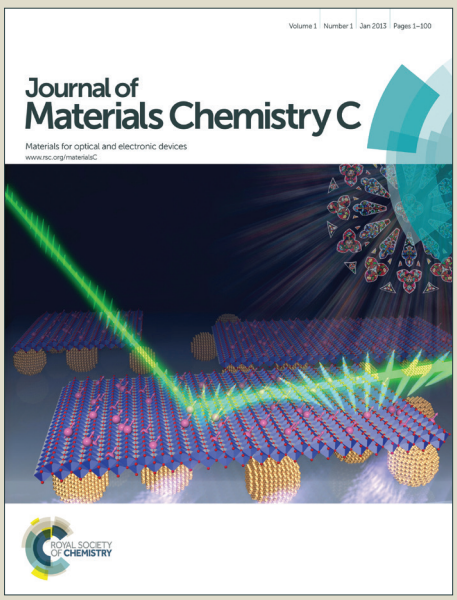

ROYAL SOCIETY OF CHEMISTRY

www.rsc.org/materialsC

Journal of Materials Chemistry C RSCPublishing

PAPER

Electrochemical luminescence modulation in a Eu(III) complex-modified TiO_2 electrode

Cite this: DOI: 10.1039/x0xx00000x

Kenji Kanazawa,[a] Kazuki Nakamura and Norihisa Kobayashi*

Received 00th January 2012,
Accepted 00th January 2012

DOI: 10.1039/x0xx00000x

www.rsc.org/

Electrochemical modulation of red luminescence from a europium(III) complex was demonstrated. In order to elucidate the mechanism of luminescence modulation, cyclic voltammogram, absorption spectra, emission spectra, emission lifetime, and emission quantum yield were measured. From these measurements, the modulation of emission was found to be achieved through an electrochemical reaction of TiO_2 that is facilitated by electron transfer between the europium(III) complex and TiO_2. Subsequent immobilization of the europium(III) complex on a TiO_2 electrode achieved an on-off emission contrast of 74:1, with the response time and repetition stability of emission switching being considerably improved.

1. Introduction

Luminescent lanthanide(III) [Ln(III)] complexes have long been regarded as attractive luminescent molecules for a widespread range of applications, but particularly as phosphors, bioassays, and for sensor development by virtue of their unique optical properties such as narrow emission bands, long luminescence lifetimes, and high transparency in the visible region (i.e., a large Stokes shift).[1-10] More recently, Ln(III) complexes exhibiting reversible luminescence triggered by external photo-, thermal-, and electric- stimuli have attracted particular attention due to their potential to be used in chemical/biochemical sensors, molecular logic gates, molecular memories, and display devices. For example, Kawai et al. have reported that europium [Eu(III)] complexes in which photochromic terarylene or diarylethene derivatives function as the photoresponsive ligand can achieve relatively high photochromic performance when used as a photoswitching unit.[11-13] In such a system, the emission intensity of the Eu(III) complex reversibly changes when its photochromic unit is converted from a colorless open-ring form to a colored closed-ring through irradiation with ultraviolet (UV) light. This change in emission intensity is attributed not only to the intramolecular fluorescence resonance energy transfer (FRET), but also to a change in the symmetry of the coordination structure around Eu(III) center. A thermo-sensitive material based on lanthanide coordination polymers composed of terbium [Tb(III)] and Eu(III) complexes has been reported by Hasegawa et al. to exhibit remarkable emission properties across a wide temperature range of 200-500 K, which includes a change in color from green, to yellow, orange, and red in response to temperature due to intermolecular FRET between the Tb(III) and Eu(III) ions.[14] The authors of this paper have also reported a polymeric composite material based on a fluoran dye, a suitable developer and a luminescent Eu(III) complex; the emission intensity of Eu(III) complex could be reversibly changed via the thermochromic reaction taking place within the fluoran dye-developer system.[15] In other words, photoluminescence could be modulated through the intermolecular FRET between the excited Eu(III) ions and colored fluoran dye.

Of the various external stimuli that can be used, we have opted to focus on the electrochemically-triggered luminescence of Eu(III) complexes based on the fact that this can be applied rapidly and reversibly. In previous research, we reported that the electrochemical luminescence of an Eu(III) complex can be modulated by an electrochemical cell incorporating a diheptyl viologen (HV^{2+}) solution and/or a Prussian blue (PB) modified electrode. We investigated the electroswitchable photophysical properties that were achieved by combining photoluminescent and electrochemically active molecules.[16-19] However, most of these systems[20-21] (including our systems)[16-19,22] do not usually exhibit a sufficiently rapid response, high reversibility, or high on-off fluorescence modulation contrast, which are all requirements for long-term application. That is, the fluorescence modulation response is dependent on the FRET or electron transfer between luminescent and electrochemically active molecules that is induced by an electrochemical redox reaction.

In order to achieve a rapid fluorescence modulation response, it is necessary to immobilize both luminescent and electrochemically active molecules on the same electrode; in

particular, immobilizing molecules on an electrode is a powerful method to decrease the time of electrochemical reaction.[23-26] Various methods of achieving this immobilization have been reported, but most have typically been based on FRET from a host material such as nanocrystalline titania microspheres,[27-30] clay[31-33] and zeolite[34-37] to luminescent species such as Eu(III) ion. However, the lower energy transfer efficiency of these materials makes it difficult to achieve a large on-off emission contrast.

In order to increase the rate of response and on-off emission contrast of Eu(III) luminescence, we herein focus on the immobilization of a novel Eu(III) complex on a titanium oxide (TiO_2) nanoparticle-modified electrode. A TiO_2 film is chosen since it offers a large surface area for the adsorption and reaction between adsorbed molecules and TiO_2, which have already been widely used in applications such as dye-sensitized solar cells[38-43] and electrochromic displays.[39,44-48] The immobilization of an Eu(III) complex on a TiO_2 electrode is therefore expected to increase the fluorescence intensity, as the typically high molecular extinction coefficient of antenna ligands in the Eu(III) complex allows them to effectively transfer energy to Eu(III) ions, leading to a high contrast emission modulation.

2. Experimental Section

2.1 Materials

Europium(III) chloride hexahydrate ($EuCl_3 \cdot 6H_2O$; 99.9 %), ethanol (EtOH), methanol (MeOH) and *N,N*-dimethylformamide (DMF) were all purchased from Wako Pure Chemical Industries Ltd. Further, 4,4,4-trifluoro-1-(2-thienyl)-1,3-butanedione (tta), 2,2'-bipyridine-4,4'-dicarboxylic acid (H_2dcbpy), and ferrocene (Fc) were purchased from Tokyo Chemical Co. Inc., and used as received. Sodium hydroxide (NaOH) (Kanto Chemical Co. Inc.) was used to remove a proton of tta. A nanocrystalline TiO_2 paste (PST-18NR) used to fabricate the electrode was purchased from JGC Catalysts and Chemicals Ltd. Lithium perchlorate ($LiClO_4$) (Wako Pure Chemical Industries) was used as a supporting electrolyte without further purification. Propylene carbonate (PC) (Kanto Chemical Co. Inc.) was used as a solvent after first removing any water by molecular sieves (Kanto Chemical Co. Inc.). An indium tin oxide (ITO) glass electrode (Yasuda, 10 Ω/sq) was also obtained and prepared by washing with detergent in an ultrasonic bath, followed by cleaning in deionized water twice, and then in acetone (each sequence lasting 20 min).

2.2 Characterization

Infrared (IR) spectra were recorded on a JASCO FT/IR-660 Plus infrared spectrometer using the KBr method. High-resolution mass spectroscopy (HRMS) was using a Thermo Scientific Exactive apparatus, while elemental analysis of C, H, and N was performed using Perkin-Elmer 2400. The elemental composition of the $Eu(tta)_3$dcbpy-modified TiO_2 electrode was determined using a scanning electron microscope (SEM, JEOL JSM-6510A) equipped with an energy-dispersive X-ray spectroscope (EDS, JSM-6510LA)

2.3 Synthesis of a diaquatris(thenoyltrifluoroacetonate)europium(III) $[Eu(tta)_3(H_2O)_2]$ complex

In a 500 mL flask, 4,4,4-trifluoro-1-(2-thienyl)-1,3-butanedione (tta) (1.33 g, 6 mmol) was first dissolved in 30 mL ethanol. And then, both NaOH (1 N, 6 mL) and a solution of $EuCl_3 \cdot 6H_2O$ (0.73 g, 2 mmol) in 10 mL of water were successively added to the tta solution. Next, an additional 200 mL of water was added, and the mixture was heated at reflux while stirring for 12 h. The complex precipitated during cooling to room temperature was filtered off, washed with water and then dried in a vacuum. The solid product obtained was then recrystallized from methanol/water to produce a pale-yellow solid with a yield of 1.06 g (62 %). IR (KBr, cm^{-1}): 1604 (C=O stretch), 1584 (C=C stretch), 1542 (C=C stretch); HRMS (ESI): m/z calcd for $C_{24}H_{13}O_6EuF_9S_3$ $[M-2H_2O+H]^+$: 816.8937; found: 816.8943; elemental analysis calcd (%) for $C_{24}H_{16}EuF_9O_8S_3$: C, 33.85, H, 1.89; found: C, 34.03, 2.05.

2.4 Preparation of TiO_2 electrodes

Thoroughly washed ITO glass electrodes were further cleaned with UV-O_3 for 40 min to ensure the complete removal of all organic substances. Onto this, the TiO_2 paste was cast using a glass rod technique, then allowed to dry in ambient atmosphere for 2 h. After further drying at 90 °C for 1 h, sintering at 450 °C for 1 h, and then cooling to room temperature. A final film thickness of about 8.0 ± 0.2 μm was obtained.

2.5 Preparation of a $Eu(tta)_3$dcbpy layer on TiO_2-ITO glass electrodes

A modified Eu(III) complex on a TiO_2 electrode was prepared according to previous reports.[24,46-52] After cleaning the TiO_2 coated ITO electrode with UV-O_3 for 20 minutes to remove any organic substances, it was immersed in DMF solution containing 0.5 mM of H_2dcppy at room-temperature for 24 h. The electrode was then rinsed with DMF to remove any unreacted residue and dried under vacuum for 24 h at room temperature. This modified electrode was then immersed in boiled MeOH solution containing 1 mM of $Eu(tta)_3(H_2O)_2$ for 24 h. Finally, the modified electrode was rinsed thoroughly with MeOH to remove any unreacted residue, and then dried at room temperature under vacuum for 24 h to remove any residual solvent. The resulting electrode structure is shown schematically in Fig. 1.

2.6 Electrochemical measurement

Cyclic voltammograms (CVs) and chronoamperometric measurements were recorded on a potentiostat/galvanostat (ALS, 660A) equipped with a computer. For this, a three-electrode cell was constructed with an ITO-glass working electrode (reaction area of 2 cm^2), a Pt wire counter electrode and an Ag/AgCl reference electrode. The electrolyte solution was prepared by dissolving $LiClO_4$ (200 mM) in PC, and was

purged with nitrogen gas for 20 min prior to each experiment. The absorption spectra for this three-electrode cell were recorded in situ by applying a potential between 0 and -0.8 V (vs. Ag/AgCl) at a scan rate of 50 mV/s using a diode array detection system (Ocean Optics, USB2000).

2.7 Photophysical measurement

Ultraviolet-visible (UV-vis) absorption spectra for the three-electrode cell containing $LiClO_4$ (200 mM) in PC were measured using a spectrophotometer (JASCO, V-570) and quartz cells with a 10 mm long optical path. Photo luminescence spectra were obtained at an excitation wavelength of 377 nm using a spectrofluorometer (JASCO, FP-6600). The quantum yields of the $Eu(tta)_3(H_2O)_2$ solution in a quartz cell with a 1.0 mm long optical path, a $Eu(tta)_3$dcbpy-modified TiO_2 electrode and a $Eu(tta)_3$dcbpy-modified TiO_2 electrode immersed in PC electrolyte solution (path length of 10 mm) were determined by standard procedures with an integral sphere (JASCO ILF-533, diameter 10 cm) mounted on a spectrofluorometer (JASCO FP-6600). The excitation wavelengths used for the $Eu(tta)_3(H_2O)_2$ solution and $Eu(tta)_3$dcbpy-modified electrode were 337 and 377 nm, respectively. Measurement of emission lifetime was carried out using a N_2 laser with 4 ns pulse width at 337 nm (Spectra-Physics, VSL-337) and a photomultiplier (Hamamatsu photonics, H10721-20MOD, response time 0.8 ns). Emission decays were monitored with a digital oscilloscope (Sony Tektronix TDS3052, 500 MHz) synchronized to single-pulse excitation. The emission decay curves were analyzed by single or bi- exponential curve fitting. All solutions used for optical measurement were purged with nitrogen gas for 20 min prior to each experiment.

3. Results and Discussion

3.1 Elemental composition of $Eu(tta)_3$dcbpy-modified TiO_2 electrodes

In order to analyze the elemental composition of the $Eu(tta)_3$debpy-modified TiO_2 electrode, SEM-EDS measurement was performed. Small Eu, S, and C peaks in combination with large Ti and O peaks were observed in the EDS spectrum (Fig. S1). The elemental ratio of Eu, Ti, and O were found to be 0.73, 23.97, 61.30 %, respectively (Table S1).

3.2 FT-IR spectra of modified electrodes

The $Eu(tta)_3$dcbpy complex was confirmed to be covalently-immobilized onto the TiO_2 electrode through IR measurements. The TiO_2-based film samples were peeled and held between KBr plates. Other powder samples were treated in the same manner. From the results shown in Fig. 2, there are clearly no obvious peaks between 2000 and 1000 cm^{-1} for the TiO_2 film. The two broad bands observed at 1604 and 1366 cm^{-1} for H_2dcbpy are assigned to the asymmetric and symmetric stretching modes of carboxylate groups. In dcbpy-immobilized TiO_2, these peaks of carboxylate symmetric-stretching vibrations shifted to 1598 and 1382 cm^{-1}, indicating that the carboxylic group of H_2dcbpy was dissociated and adsorbed onto the TiO_2 surface. However, following modification by the $Eu(tta)_3(H_2O)_2$ complex, strong peaks originating from the Eu(III) complex are seen at 1604 (tta: C=O stretch), 1584 (tta: C=C stretch), and 1542 (tta: C=C stretch) cm^{-1}. These peaks imply that $Eu(tta)_3$dcbpy is successively connected to the TiO_2 electrode.

The IR spectra also provide an indication of the mechanism by which the carboxylate binds to the TiO_2 electrode. Specifically, the values for the frequency difference $\Delta\upsilon$ ($\Delta\upsilon = \upsilon_{asym\cdot COO^-} - \upsilon_{sym\cdot COO^-}$) between non-symmetric and symmetric COO^- stretching bands observed at 216 cm^{-1} for H_2dcbbpy anchored on TiO_2 and 238 cm^{-1} for H_2dcbpy in KBr pellets. These results suggest that the carboxylate groups are coordinated via a bidentate chelate or bidentate bridging mode to the TiO_2 surface rather than via an ester-type linkage (Fig. 3).[46,47] Similar results have been previously observed in the case of ruthenium complexes anchored on TiO_2.[49-52]

3.3 Electrochemical properties of modified electrodes

In order to investigate the electrochemical properties of the TiO_2 electrode and $Eu(tta)_3$dcbpy-modified TiO_2 electrode, their cyclic voltammograms (CVs) and changes in absorbance at 600 nm were measured (Fig. 4(a) and (b)). This data revealed that in both electrodes there is an increase in reductive current from -0.3 V (vs. Ag/AgCl), with a slight increase in absorbance observed at 600 nm during potential scanning in the negative direction. Furthermore, when the potential was scanned from -0.8 to 0 V, an oxidative current was found at a potential of -0.61 and -0.67 V in the TiO_2 and $Eu(tta)_3$dcbpy-modified TiO_2 electrodes, respectively. As this oxidative current increased, the absorbance at 600 nm decreased and recovered to its initial state in both electrodes. The absorption spectra of the TiO_2 and $Eu(tta)_3$dcbpy-modified TiO_2 electrodes also exhibited a slight increase from 400 to 700 nm when applying a potential of -0.8 V for 5 s. Furthermore, when a potential of 0 V was applied to these cells for 10 s, the absorbance of each electrode recovered to its respective initial value. Based on this change in absorbance and the corresponding CVs, this electrochemical and optical behavior is considered to be caused by the electrochemical reduction of the TiO_2 film.

3.4 Optical properties of an $Eu(tta)_3$dcbpy-modified TiO_2 electrode

The excitation and emission spectra of the $Eu(tta)_3$dcbpy-modified TiO_2 electrode along with its change in emission intensity under an applied potential sweep to determine how the electrochemical reaction of the modified electrode affects emission from the Eu(III) complex (the measurement set up is shown in Fig. S2). As can be seen in the excitation spectrum in Fig. 5, the peak observed at around 377 nm corresponds to the absorption of tta ligands in the Eu(III) complex. When these are excited by a 377 nm light source with zero applied potential, strong red emissions are observed from the Eu(III) complex, as evidenced by the red solid line and photo in Fig. 5. The sharp emission bands that can be seen at around 580, 592, 613, 653

and 703 nm are all attributable to the intraconfigurational 4f-4f transitions of $^5D_0 \rightarrow {}^7F_J$ (J = 0, 1, 2, 3, and 4, respectively). The change in emission intensity (613 nm) of the modified electrode was also monitored under a sweeping applied potential (Fig. 6). Interestingly, when the reductive current increased from -0.24 V (vs. Ag/AgCl), the red emission intensity from Eu(III) complex decreased. Furthermore, with continuous sweeping of the potential from -0.8 V to 0 V, the red emission recovered gradually from -0.55 V in succession to the oxidative current flowed and returned to its initial value at 0 V. From these results, luminescence control would be most likely due to electrochemical reaction of TiO_2. Additionally, as shown by the change in emission intensity with the application of different potentials for 5 s (Fig. 7(a)), emission from the Eu(III) complex was completely quenched at -0.8 V (Fig. 7(b) and photo in Fig. 7(b)). The on-off emission contrast was calculated to be 74:1 (Fig. 7(b)). This high on-off rate is attributed to the immobilization of the Eu(III) complex on the TiO_2 electrode. The emission quenching efficiency (η_q) was also calculated using the following equation:

$$\eta_q = 1 - \frac{\Phi_5}{\Phi_0}$$

where ϕ_0 and ϕ_5 are the emission quantum yields before and after the application of -0.8 V for 5 s (Table 1). The estimated quenching efficiency of over 98 % suggests that emission switching was successfully achieved in the modified electrode. It also indicates that the electrochemical reaction of the Eu(tta)$_3$dcbpy-modified TiO_2 electrode discussed in the previous section greatly affects the red emission from Eu(tta)$_3$dcbpy.

In order to study the change in emission intensity at 613 nm with the application of a negative potential, and the response time of this electrochemically induced emission control, changes in the emission intensity and chronoamperometric response of the Eu(tta)$_3$dcbpy-modified TiO_2 electrode were measured under sequential application of -0.8 V (vs. Ag/AgCl) for 5 s and 0 V for 10 s. As shown in Fig. 8, the application of -0.8 V for 1 s was sufficient to reduce the initial emission intensity by up to 90 %. This rapid quenching response was again caused by the immobilization of the Eu(III) complex on the TiO_2 electrode. With subsequent removal of this applied potential, the initial emission intensity was recovered within 10 s, but up to 90 % was recovered within the first 3 s. Thus, this modified electrode exhibits luminescence modulation with a quick response. The switching behavior of the modified electrode is also shown in the movie provided as Supporting Information.

The emission lifetime of the Eu(tta)$_3$(H$_2$O)$_2$ solution (Fig. S3) and Eu(tta)$_3$dcbpy-TiO_2 electrodes (Fig. S4) with and without an electrolyte solution was measured under open circuit conditions with various durations of potential application (see Fig. S5 and S6) to elucidate the mechanism behind the electrochemically induced modulation of Eu(tta)$_3$dcbpy. Interestingly, the Eu(tta)$_3$dcbpy-modified electrode exhibited two distinct emission lifetimes from Eu(III) (τ_1, τ_2), whereas the Eu(tta)$_3$(H$_2$O)$_2$ alone had only the one component. The shorter emission of the modified electrode is most likely due to $^5D_0 \rightarrow {}^7F_J$ transitions that are affected by electron transfer from the Eu(III) complex to TiO_2, whereas the longer emission is relatively independent of electron transfer. Furthermore, as shown in Table 1, soaking the Eu(tta)$_3$dcbpy-modified electrode in electrolyte solution significantly reduced its emission lifetime when applying a potential of -0.8 V for 0.5, 1, 2, 3 and 5 s. The longer components of emission lifetimes at the open circuit and at the time after applying the potential for 0.5, 1, 2, 3 and 5 s were 227, 198, 167, 121, 64 and 26 μs, respectively; whereas the shorter ones were 46, 28, 18, 13, 9 and 1.1 μs.

The emission lifetime and the ratio of the longer emission process were both found to decrease with increasing duration of applied potential, with previous our reports[15,17,18] finding that this increase in duration dramatically reduces the quantum yield and lifetime of emission. In these previous results, however, luminescence modulation is likely the result of intermolecular FRET from the excited Eu(III) ions to electrochemically active molecules, because the emission spectra of the Eu(III) complex showed a high degree of overlap with the absorption spectra of the electrogenerated molecules. In contrast, the Eu(tta)$_3$dcbpy-modified TiO_2 electrode of the present study shows only a very small overlap, suggesting that FRET is not in fact a major factor in luminescence modulation. We therefore used UV-vis spectra (Fig. S7) and CV measurements (Fig. S8) to estimate the highest occupied molecular orbital (HOMO) and lowest unoccupied molecular orbital (LUMO) level of the tta ligands and Eu(tta)$_3$(H$_2$O)$_2$, as well as the valence band (VB) and conduction band (CB) of the TiO_2 electrode. These results are summarized in Table 2 and depicted in Fig. 9. These results revealed that the CB of TiO_2 is situated between the HOMO and LUMO of the tta ligands in Eu(III) complex.

By taking those energy levels of the Eu(III) complex and TiO_2 into consideration, we assumed the mechanism of the fluorescent switching as follows. When the reduction potential of the TiO_2 is applied to the modified electrode, electrons are injected to the CB of TiO_2, which is exiting at higher energy level than HOMO of tta ligands. By photo-excitation of tta ligands, in this situation, the electron in the CB could transfer to half-filled HOMO of photo-excited tta ligands, forming the reduced state of the Eu(tta)$_3$dcbpy. The electron in the LUMO of tta ligands, which is situated above CB of TiO_2, subsequently transfer to the CB because the reduced state of the Eu(tta)$_3$(H$_2$O)$_2$ complex is not so stable in comparison with TiO_2 and tta molecule itself (Fig. 4 and Fig. S8). As the result, the photo-exited Eu(III) complex would be returned to the ground state without radiation of light.[54] This electron transfer process is considered to be the most likely cause of the observed quenching of the red emission. In contrast, red luminescence from the Eu(III) complex was clearly observed when the reduction potential of TiO_2 was not applied. The direct photo-induced electron transfer from the half-filled LUMO of photo-excited tta ligand to CB of TiO_2, which leads to formation of oxidation state of the Eu(III) complex, would be unfavorable process. This is because electrochemical oxidation of the Eu(III) complex was not observed in the CV

measurements. Therefore, the red luminescence of the Eu(III) complex could be obtained stably without electron transfer between tta ligands and TiO_2.

Finally, to verify the stability of electrochemical emission modulation, the change in the emission intensity of the $Eu(tta)_3$dcbpy-modified TiO_2 electrode was monitored at 613 nm. As shown in Fig. 10, this change in emission intensity was found to be fairly consistent over 50 cycles, indicating that the $Eu(tta)_3$dcbpy-modified electrode has a fairy high reversible emission modulation system generated by electrochemical stimuli.

Conclusions

This study has demonstrated that the red luminescence from a $Eu(tta)_3$dcbpy-modified TiO_2 electrode can be electrochemically modulated, with a dramatic decrease in emission lifetime observed when increasing the duration of an applied potential. In this way, a high on-off emission contrast of 74:1 and emission quenching efficiency of over 98 % were achieved, with the mechanism behind this emission control considered to be electron transfer between the Eu(III) complex and TiO_2 electrode. The change in emission intensity was quite rapid, requiring only 1.0 s to decrease by 90 % of its initial value and 3.0 s to recover by the same amount; figures which remained fairly consistent over 50 cycles. This rapid response and high stability of emission modulation is again attributed to electron transfer created by immobilizing the Eu(III) complex. We believe that the results of this research will contribute to the development of new sensors, as well as display applications such as monitors, digital signs, and e-paper.

Acknowledgements

This work was partly supported by a Grant-in-Aid for Young Scientists (B) (No. 23750208 and No. 25870137) from Japan Society for the Promotion of Science (JSPS), Imahori Foundation, the Mazda Foundation, and JSPS Research Fellowships for Young Scientists. The authors would acknowledge to the Center for Analytical Instrumentation of Chiba University for measurements of mass spectra and elemental analyses.

Notes and references

Department of Image and Materials Science, Graduate School of Advanced Integration Science, Chiba University, 1-33 Yayoi-cho, Inage-ku, Chiba 263-8522, Japan. E-mail: koban@faculty.chiba-u.jp; Fax: +81-43-290-3490; Tel: +81-43-290-3458.
[a] *Research Fellow of the Japan Society for the Promotion of Science (JSPS)*

†Electronic Supplementary Information (ESI) available: Details of measurement configuration of emission decay profiles for $Eu(tta)_3(H_2O)_2$ and $Eu(tta)_3$dcbpy-modified TiO_2 electrode and the results as well as absorption spectra and CVs of tta and $Eu(tta)_3(H_2O)_2$. See DOI:10.1039/b000000x/

1 J. Kido, Y. Okamoto, *Chem. Rev.*, 2002, **102**, 2357-2368.
2 K. Nakamura, Y. Hasegawa, H. Kawai, N. Yasuda, N. Kanehisa, Y. Kai, T. Nagamura, S. Yanagida, Y. Wada, *J. Phys. Chem. A*, 2007, **111**, 3029.
3 K. Binnemans, *Chem. Rev.*, 2009, **109**, 4283-4374.
4 S. Aime, M. Botta, M. Fasano, E. Terreno, *Chem. Soc. Rev.*, 1998, **27**, 19-29.
5 D. Parker, *Cood. Chem. Rev.*, 2000, **205**, 109-130.
6 H. Tsukube, S. Shinoda, *Chem. Rev.*, 2002, **102**, 2389-2403
7 C. P. Montgomery, B. S. Murray, E. J. New, R. Pal, D. Parker, *Acc. Chem. Res*., 2009, **42**, 925-937.
8 J. Yuasa, T. Ohno, H. Tsumatori, R. Shiba, H. Kamikubo, M. Kataoka, Y. Hasegawa, T. Kawai, *Chem. Commun.*, 2013, **49**, 4604-4606.
9 L. Armelao, S. Quici, F. Barigelletti, G. Accorsi, G. Bottaro, M. Cavazzini, E. Tondello, *Cood. Chem. Rev.*, 2010, **205**, 487-505.
10 Y. Hasegawa, Y. Wada, S. Yanagida, *J. Photochem. Photobiol. C*, 2004, **5**, 183-202.
11 T. Nakagawa, K. Atsumi, T. Nakashima, Y. Hasegawa, T. Kawai, *Chem. Lett.*, 2007, **36**, 372-373.
12 T. Nakagawa, Y. Hasegawa, T. Kawai, *J. Phys. Chem. A*, 2008, **112**, 5096-5103.
13 T. Nakagawa, Y. Hasegawa, T. Kawai, *Chem. Commun.*, 2009, **37**, 5630-5632.
14 K. Miyata, Y. Konno, T. Nakanishi, M. Kato, K. Fushimi, Y. Hasegawa, *Angew. Chem., Int. Ed.*, 2013, **52**, 6413-6416.
15 K. Nakamura, Y. Kobayashi, K. Kanazawa, N. Kobayashi, *J. Mater. Chem. C*, 2013, **1**, 617-620.
16 K. Nakamura, K. Kanazawa, N. Kobayashi, *Chem. Commun.*, 2011, **47**, 10064-10066.
17 K. Kanazawa, K. Nakamura, N. Kobayashi, *Chem. –Asian J.*, 2012, **7**, 2551-2554.
18 K. Kanazawa, K. Nakamura, N. Kobayashi, *Jpn. J. Appl. Phys.*, 2013, **52**, 05DA14.
19 K. Nakamura, K. Kanazawa, N. Kobayashi, *Displays*, 2013, **34**, 389-395.
20 M. Yano, K. Matsuhira, M. Tatsumi, Y. Kashiwagi, M. Nakamoto, M. Oyama, K. Ohkubo, S. Fukuzumi, H. Misaki, H. Tsukube, *Chem. Commun.*, 2012, **48**, 4082-4084.
21 T. Sato, M. Higuchi, *Chem. Commun.*, 2013, **49**, 5256-5258.
22 K. Kanazawa, K. Kanazawa, K. Nakamura, N. Kobayashi, *J. Phys. Chem. A*, 2014, **118**, 6026-6033.
23 J. Malinge, C. Allain, L. Galmiche, F. Miomandre, P. Audebert, *Chem. Mater*., 2011, **23**, 4599-4605.
24 S. Seo, H. Allain, J. Na, S. Kim, X. Yang, C. Park, J. Malinge, P. Audebert, E. Kim, *Nanoscale*, 2013, **5**, 7321-72327.
25 H. Gu, L. Bi, Y. Fu, N. Wang, S. Liu, Z. Tang, *Chem. Sci.*, 2013, **4**, 4371-4377.
26 X. Yang, S. Seo, C. Park, E. Kim, *Macromolecules*, 2014, **47**, 7043-7051.
27 E. J. Nassar, R. R. Goncalves, M. Ferrari, Y. Messaddeq, S. J. L. Ribeiro, *J. Alloys. Compd.*, 2002, **344**, 221-225.
28 M. Tan, G. Wang, Z. Ye, J. Yuan, *J. Lumin.*, 2006, **117**, 20-28.

29 L. A. Rocha, K. L. Cluffi, H. C. Sacco, E. J. Nassar, *Mater. Chem. Phys.*, 2004, **85**, 245-250.
30 X. –L. Wang, B. Yan, *Colloid Polym. Sci.*, 2011, **289**, 423-431
31 S. Celedon, C. Quiroz, C. M. Sotomayor Torres, E. Benavene, *Mater. Res. Bull.*, 2009, **44**, 1191-1194.
32 M. Lezhnina, E. Benavente, M. Bentlage, Y. Echevarria, E. Klumpp, U. Kynast, *Chem. Mater.*, 2007, **19**, 1098-1102.
33 Y. Ma, H. Wang, W. Liu, Q. Wang, J. Xu, Y. Tang, *J. Phys. Chem. B*, 2009, **113**, 14139-14135.
34 Y. Wada, M. Sato, Y. Hasegawa, *Angew. Chem., Int. Ed.*, 2006, **45**, 1925-1928.
35 Y. Wang, H. Li, L. Gu, Q. Gan, Y. Li, G. Calzaferri, *Micrporous Mesoporous Mater.*, 2009, **121**, 1-6.
36 P. Li, Y. Zhang, Y. Wang, Y. Wang, H. Li, *Chem. Commun.*, 2014, **50**, 13680-13682.
37 Y. Wang, H. Li, *CrystEngComm*, 2014, **16**, 9764-9778.
38 B. O'Regan. M. Grätzel, *Nature*, 1991, **353**, 737-740.
39 X. Chen, S. S. Mao, *Chem. Rev.*, 2007, **107**, 2891-2959.
40 S. Ardo, G. J. Meyer, *Chem. Soc. Rev.*, 2009, **38**, 115-164.
41 M. Grätzel, *Acc. Chem. Res.*, 2009, **42**, 1788-1798.
42 H. Imahori, T. Umemiya, S. Ito, *Acc. Chem. Res.*, 2009, **42**, 1809-1818.
43 A. Hagfeldt, G. Boschloo, L. Sun, L. Kloo, H. Pettersson, *Chem. Rev.*, 2010, **110**, 6595-6663.
44 D. Cummins, G. Boschloo, M. Ryan, D. Corr, S. N. Rao, D. Fitzmaurice, *J. Phys. Chem. B*, 2000, **104**, 11449-11459.
45 U. Bach, D. Corr, D. Lupo, F. Pichor. M. Ryan, *Adv. Mater.*, 2002, **14**, 845-848.
46 D. Corr, U. Bach, D. Fay, M. Kinsella, C. McAtamney, F. O'Reilly, S. N. Rao, N. Stobie, *Solid State Ionics*, 2003, **165**, 315-321.
47 C. Ma, M. Taya, C. Xu, *Electrochim. Acta*, 2008, **54**, 598-605.
48 M. Freitag, E. Galoppini, *Langmuir*, 2010, **26**, 8262-8269.
49 K. S. Finnie, J. R. Bartlett, J. L. Woolfrey, *Langmuir*, 1998, **14**, 2744-2749.
50 K. Suto, A. Konno, Y. Kawata, S. Tasaka, A. Sugita, *Chem. Phys. Lett.*, 2012, **536**, 45-49.
51 Z. Zhang, S. M. Zakeeruddin, B. C. O'Regan, R. Humphry-Baker, M. Grätzel, *J. Phys. Chem. B*, 2005, **109**, 21818-21824.
52 S. –H. Fan, A. –G. Zhang, C. –C. Ju, L. –H. Gao, K. –Z. Wang, *Inorg. Chem.*, 2010, **49**, 3752-3763.
53 M. Grätzel, *Nature*, 2001, **414**, 338-344.
54 K. Szacilowski, *Chem. Rev.*, 2008, **108**, 3481-3548.

Journal of Materials Chemistry C RSCPublishing

PAPER

List of tables

Table 1. Emission quantum yields (ϕ) and emission lifetimes (τ) of the samples.

	State	Potential [V]	ϕ [%]	τ_1 [μs]	τ_2 [μs]
$Eu(tta)_3(H_2O)_2$	Solution	Open	26	553	–
$Eu(tta)_3$dcbpy—TiO_2 [a]	Without electrolyte solution	Open	3.7	65±1.66 (40 %) [b]	225±1.89 (60 %) [c]
$Eu(tta)_3$dcbpy—TiO_2 [a]	In electrolyte solution	Open	1.8	46±3.91 (42 %) [b]	227±4.63 (58 %) [c]
$Eu(tta)_3$dcbpy—TiO_2 [a]	In electrolyte solution	-0.8	< 0.03	1.1±0.07 (69 %) [b]	26±0.60 (31 %) [c]

[a]Modified on ITO electrode. The emission decay curves were analyzed using a biexponential curve fitting of $[I(t) = A_1\exp(-t/\tau_1) + A_2\exp(-t/\tau_2)]$. [b]The value in parentheses represents $A_1/(A_1+A_2)$. [c]The value in parentheses represents $A_2/(A_1+A_2)$. All parameters of the modified electrodes are given in Fig. S4 and S6.

Table 2. Optical and electrochemical properties of the compounds.

Compd.	$\lambda_{max,abs}$ [nm]	$\varepsilon_{max,abs}$ [$mol^{-1}Lcm^{-1}$]	$\lambda_{onset,abs}$ [nm]	$E_{red,onset}$ [a] [V]	HOMO [b] [eV]	LUMO [c] [eV]	E_g [d] [eV]
TiO_2 electrode	–	–	388 [e]	-0.30	-7.30	-4.10	3.20 [e]
tta	330	18641	412	-0.55	-6.86	-3.85	3.01
$Eu(tta)_3(H_2O)_2$	339	55796	404	-0.79	-6.68	-3.61	3.07

[a]Potentials determined from the CVs of the samples vs. Ag/AgCl in a $LiClO_4$/PC solution at a scan rate of 50 mVs^{-1}. [b]HOMO = LUMO – E_g. [c]Calculated using LUMO = $[-(E_{red,onset} - 0.40) - 4.8]$ eV, where 0.40 V is the half-wave potential of Fc/Fc^+ in $LiClO_4$/PC solution and 4.8 eV is the energy level of Fc under vacuum. [d]HOMO–LUMO gap (E_g), as estimated from $\lambda_{onset,abs}$: $E_g = 1240/\lambda_{onset,abs}$. [e]Reference.[53]

Figure captions

Fig. 1 Schematic showing the formation of a Eu(III) complex-modified TiO_2 electrode.

Fig. 2 FT-IR spectra of (a) TiO_2, H_2dcbpy, H_2dcbpy, (b) dcbpy-modified TiO_2, $Eu(tta)_3(H_2O)_2$ and (c) $Eu(tta)_3$dcbpy-modified TiO_2.

Fig. 3 Three possible models for chemisorption of H_2dcbpy carboxylate groups onto a nanoporous TiO_2 surface: (a) monodenate ester-like, (b) bidentate chelate and (c) bidentate bridging, respectively.

Fig. 4 Changes in absorbance at 600 nm (top), cyclic voltammograms (bottom) of (a) TiO_2 and (b) a $Eu(tta)_3$dcbpy-modified TiO_2 electrode in PC solution with 200 mM $LiClO_4$. Scan rate: 50 mV/s.

Fig. 5 Excitation (blue solid line) and emission spectra (red solid line: 0 V for 10 s) of a $Eu(tta)_3$dcbpy-modified TiO_2 electrode in PC solution with 200 mM $LiClO_4$. Photographs show the changes in emission with electrochemical reaction under UV light (365 nm).

Fig. 6 Change in emission intensity at 613 nm (top) and CV (bottom) at a scan rate of 50 mV/s of a $Eu(tta)_3$dcbpy-modified TiO_2 electrode in PC solution with 200 mM $LiClO_4$. Excitation wavelength was 377 nm.

Fig. 7 (a) Emission intensity with the application of different potentials for 5 s. (b) Emission spectra (red solid line: 0 V for 10 s, black dashed line: -0.8 V for 5 s) of a $Eu(tta)_3$dcbpy-modified TiO_2 electrode in PC solution with 200 mM $LiClO_4$. The excitation wavelength was 377 nm. Photographs show the change in emission with electrochemical reaction under UV light (365 nm).

Fig. 8 Change in emission intensity at 613 nm (top) and chronoamperometric curve (bottom) of a $Eu(tta)_3$dcbpy-modified TiO_2 electrode in PC solution with 200 mM $LiClO_4$ at an applied potential of -0.8 V (vs. Ag/AgCl) for 5 s, followed by 0 V for 10 s.

Fig. 9 Energy diagram for a $Eu(tta)_3$dcbpy-modified TiO_2 electrode.

Fig. 10 Change in emission intensity at 613 nm (top) and current (bottom) of a $Eu(tta)_3$dcbpy-modified TiO_2 electrode in PC solution with 200 mM $LiClO_4$ during a subsequent double-potential step between -0.8 and 0 V for 5 and 10 s.

Fig. 1 Kenji Kanazawa et al.

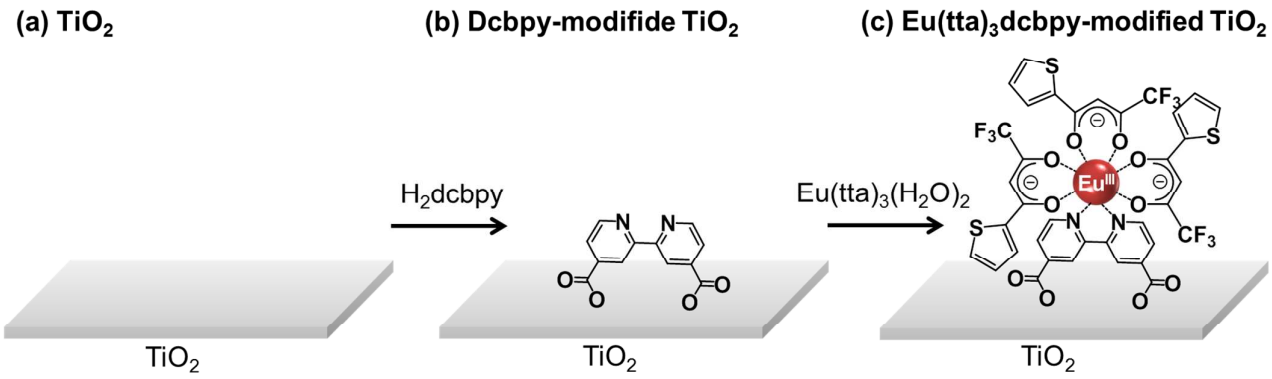

Fig. 2 Kenji Kanazawa et al.

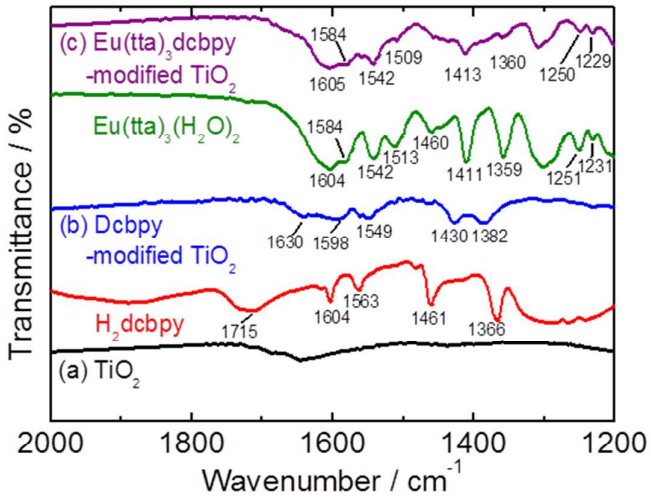

Fig. 3 Kenji Kanazawa et al.

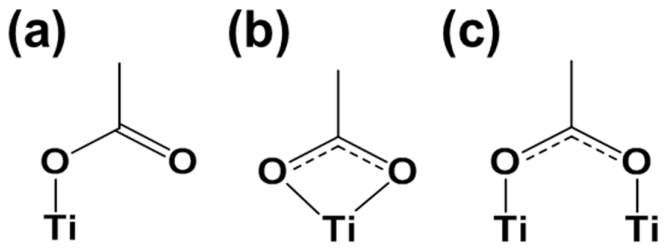

Fig. 4 Kenji Kanazawa et al.

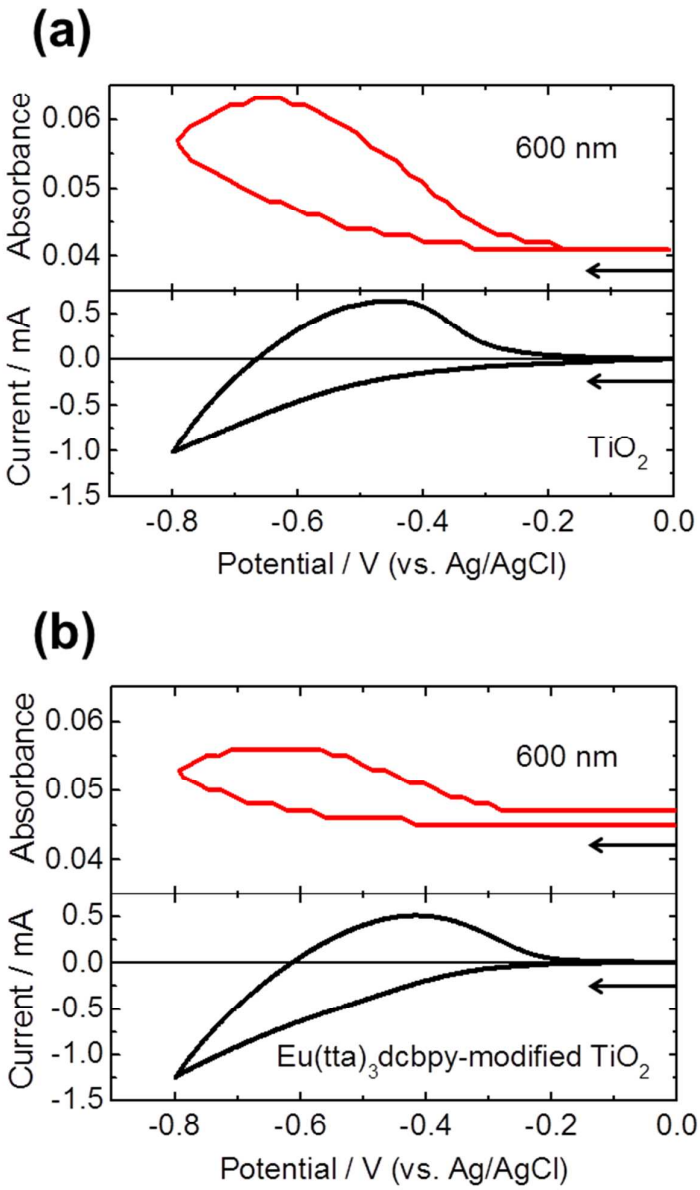

Fig. 5 Kenji Kanazawa et al.

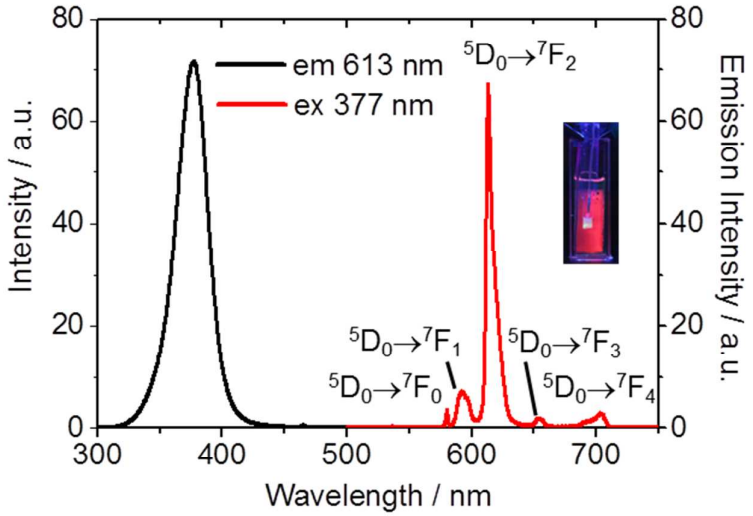

Fig. 6 Kenji Kanazawa et al.

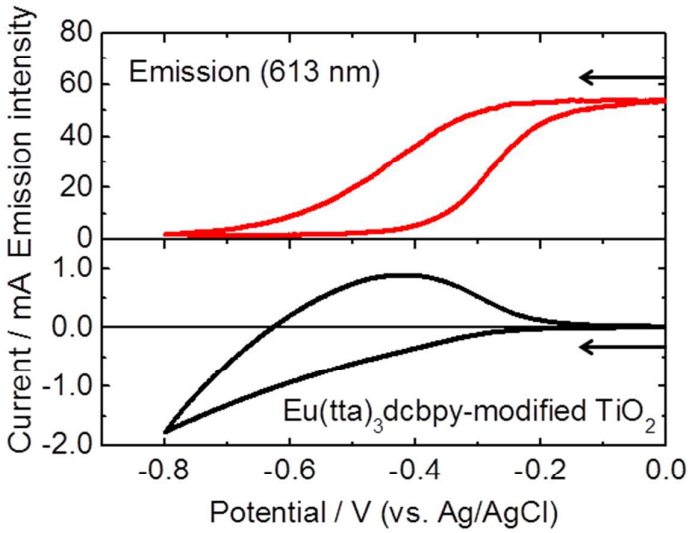

Fig. 7 Kenji Kanazawa et al.

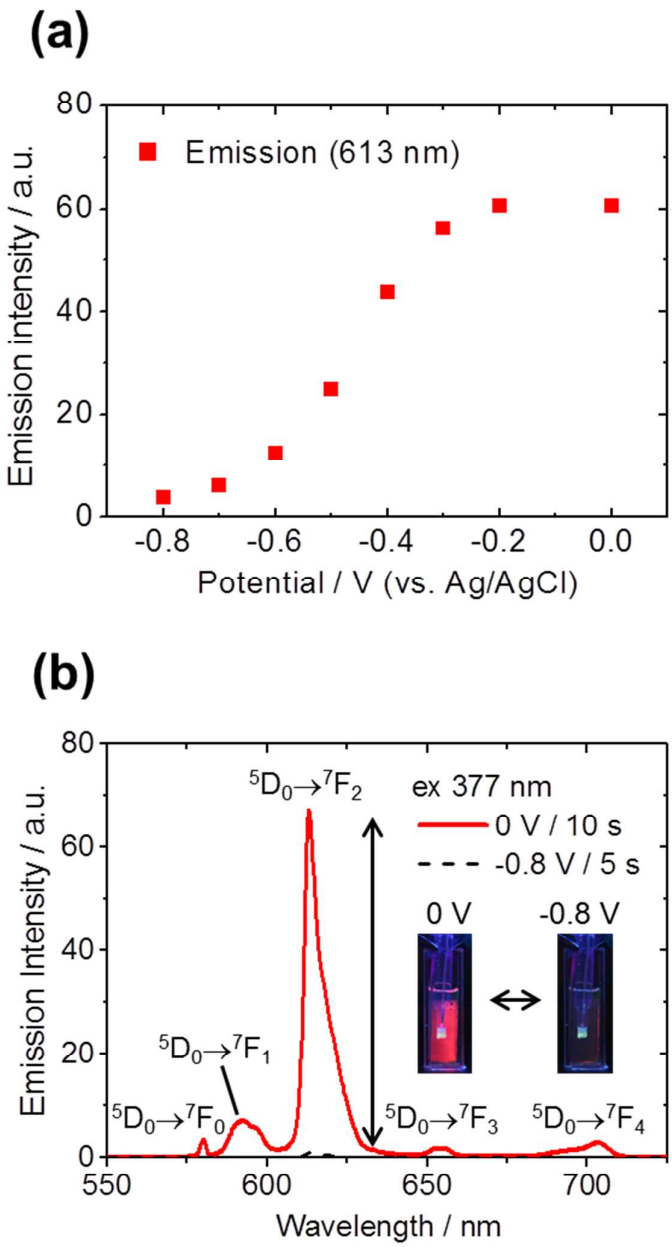

Fig. 8 Kenji Kanazawa et al.

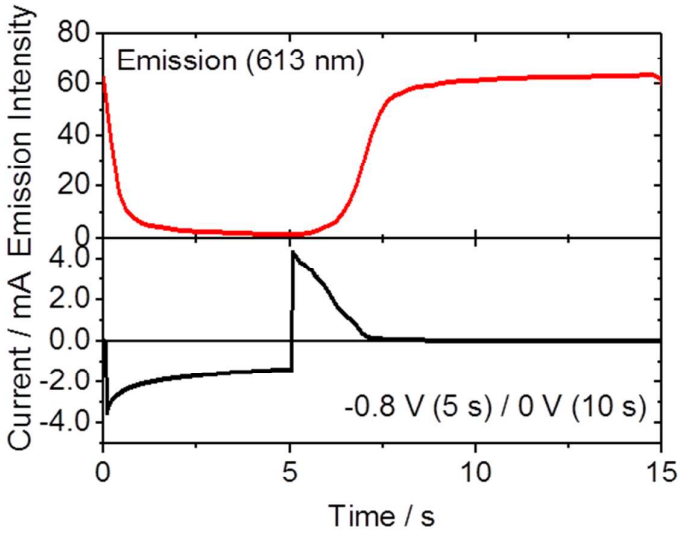

Fig. 9 Kenji Kanazawa et al.

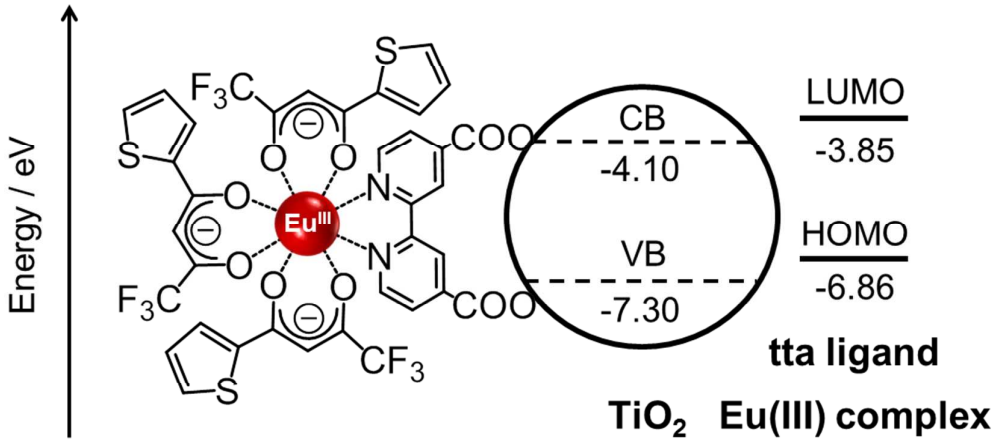

Fig. 10 Kenji Kanazawa et al.

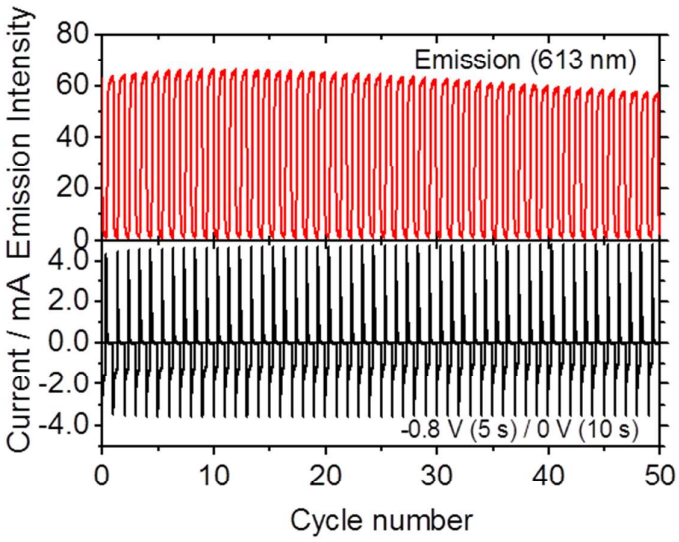

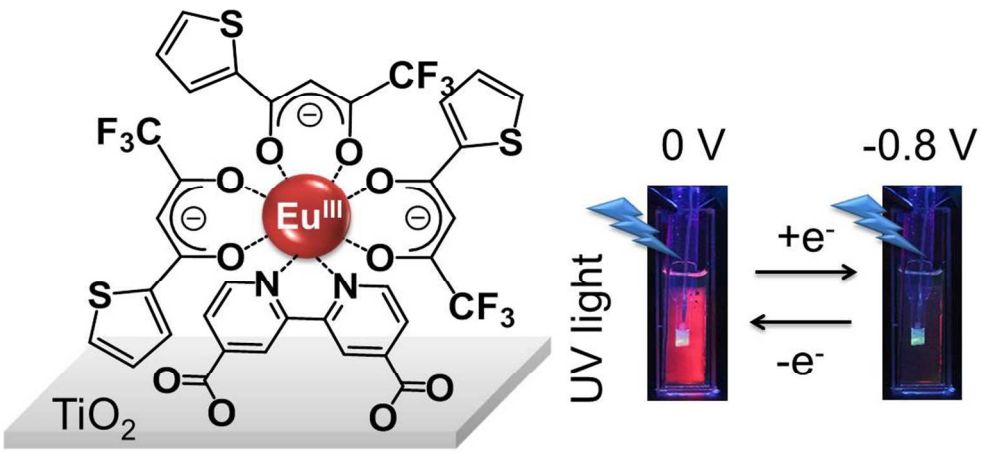

196x90mm (150 x 150 DPI)